

# B7-H3-Targeted CAR-T Cells Exhibit Potent Antitumor Effects on Hematologic and Solid Tumors

Zongliang Zhang,<sup>1,5</sup> Caiying Jiang,<sup>2,5</sup> Zhiyong Liu,<sup>3,5</sup> Meijia Yang,<sup>1</sup> Xin Tang,<sup>3</sup> Yuelong Wang,<sup>3</sup> Meijun Zheng,<sup>4</sup> Jianhan Huang,<sup>3</sup> Kunhong Zhong,<sup>1</sup> Shasha Zhao,<sup>1</sup> Mei Tang,<sup>1</sup> Tingyue Zhou,<sup>1</sup> Hui Yang,<sup>4</sup> Gang Guo,<sup>1</sup> Liangxue Zhou,<sup>3</sup> Jianguo Xu,<sup>3</sup> and Aiping Tong<sup>1</sup>

<sup>1</sup>State Key Laboratory of Biotherapy, West China Hospital, West China Medical School, Sichuan University, Chengdu, Sichuan Province, China; <sup>2</sup>Life Science and Clinical Research Center, Affiliated Hospital of Youjiang Medical University for Nationalities, Baise, Guangxi Province, China; <sup>3</sup>Department of Neurosurgery, West China Hospital, West China Medical School, Sichuan University, Chengdu, Sichuan Province, China; <sup>4</sup>Department of Otolaryngology, Head and Neck Surgery, West China Hospital, West China Medical School, Sichuan University, Chengdu, Sichuan Province, China

Recently, B7-H3 was frequently reported to be overexpressed in various cancer types and has been suggested to be a promising target for cancer immunotherapy. In the present study, we analyzed the mRNA expression of B7-H3 in The Cancer Genome Atlas (TCGA) database and validated its expression across multiple cancer types. We then generated a novel B7-H3-targeted chimeric antigen receptor (CAR) and tested its antitumor activity both *in vitro* and *in vivo*. The B7-H3 expression heterogeneity and variation were frequent. Moderate or even high expression levels of B7-H3 were also observed in some tumor-adjacent tissues, but the staining intensity was weaker than that in tumor tissues. B7-H3 expression was absent or very low in normal tissues and organs. Flow cytometry indicated that the mean expression level of B7-H3 in eight bone marrow specimens from patients with acute myeloid leukemia (AML) was 57.2% (range 38.8–80.4). Furthermore, we showed that the B7-H3-targeted CAR-T cells exhibited significant antitumor activity against AML and melanoma *in vitro* and in xenograft mouse models. In conclusion, although B7-H3 represents a promising pan-cancer target, and B7-H3-redirection CAR-T cells can effectively control tumor growth, the expression heterogeneity and variation have to be carefully considered in translating B7-H3-targeted CAR-T cell therapy into clinical practice.

## INTRODUCTION

Adoptive cell therapy (ACT) is considered to be one of the most effective immunotherapy methods for cancer treatment. One of the main ACT approaches is to use T cells engineered with chimeric antigen receptors (CARs), also known as CAR-T cells.<sup>1</sup> CARs are recombinant receptors comprising an extracellular, antigen-specific, single-chain variable fragment (scFv) fused with intracellular T cell-activating and -costimulatory signaling domains, which provide both antigen-binding sites and T cell-activating functions.<sup>2</sup> CARs

can recognize tumor antigens specifically, trigger T cell activation in a non-major histocompatibility complex (MHC)-restricted manner, and initiate an extraordinary anti-tumor response.<sup>3</sup> Cluster of differentiation (CD)19-targeting CAR-T cell therapy has been successful in the treatment of refractory/relapsed B cell malignancies, and the therapy was approved by the US Food and Drug Administration (FDA).

Despite the success of the use of CAR-T cells in the treatment of hematological tumors, their role in treating solid tumors is limited.<sup>4</sup> For hematological malignancies, lineage markers, such as the B cell marker CD19, can be targeted without serious complications caused by depletion of normal CD19<sup>+</sup> B cells. However, when treating solid cancers with engineered T cells, the identification of truly tumor-specific surface targets remains a major barrier. Targeting molecules expressed by both tumor and normal cells can cause life-threatening toxicity, as observed in clinical trials with CAR-T cells targeting human epidermal growth factor receptor 2 (HER2) because of the recognition of cognate antigen on the lung epithelium.<sup>5</sup>

B7-H3 (CD276) is a type I transmembrane protein that belongs to the B7 family.<sup>6</sup> Although B7-H3 was originally reported as a positive costimulator of T cells in humans,<sup>7</sup> increasing evidence suggests that it may be a negative regulator.<sup>8–10</sup> So far, the receptor for B7-H3 was

Received 5 March 2020; accepted 27 March 2020;  
<https://doi.org/10.1016/j.omto.2020.03.019>.

<sup>5</sup>These authors contributed equally to this work.

**Correspondence:** Aiping Tong, PhD, State Key Laboratory of Biotherapy, West China Hospital, West China Medical School, Sichuan University, Chengdu, Sichuan Province, China

**E-mail:** [aipingtong@scu.edu.cn](mailto:aipingtong@scu.edu.cn)

**Correspondence:** Jianguo Xu, MD, PhD, Department of Neurosurgery, West China Hospital, West China Medical School, Sichuan University, Chengdu, Sichuan Province, China

**E-mail:** [jianguo\\_1229@sina.com](mailto:jianguo_1229@sina.com)



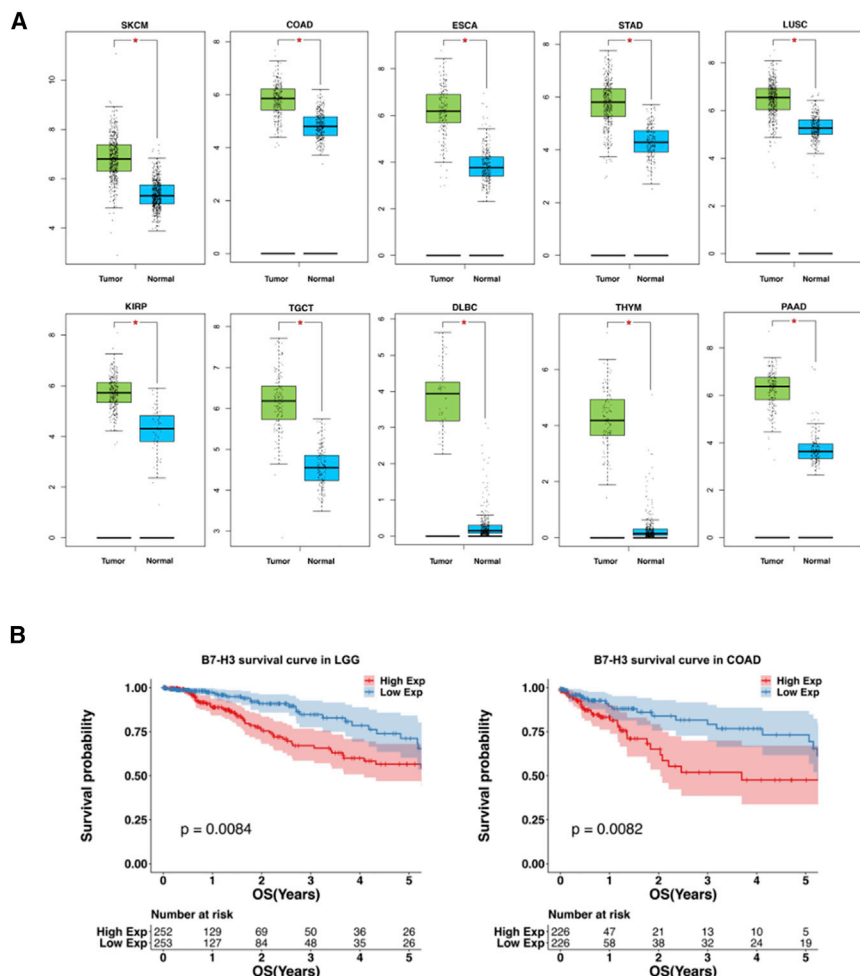


**Figure 1. Analysis of B7-H3 Expression and Survival in TCGA Database**

(A) Normalized mRNA levels of *CD276* in tumor and normal tissues using the online web server GEPIA. SKAM, skin cutaneous melanoma; COAD, colon adenocarcinoma; ESCA, esophageal carcinoma; STAD, stomach adenocarcinoma; LUSC, lung squamous cell carcinoma; KIRP, kidney renal papillary cell carcinoma; PAAD, pancreatic adenocarcinoma; TGCT, testicular germ cell tumors; DLBC, diffuse large B cell lymphoma; THYM, thymoma. (B) Correlational analysis between overall survival time and B7-H3 expression level in LGG and COAD by GEPIA. Each point represents a different TCGA sample. More analysis results are provided in Figures S1 and S2. \* $p < 0.05$ .

developed by MacroGenics, because of liver toxicity events in the monotherapy trial, including reversible elevation of transaminase levels with or without concurrent elevation of bilirubin level.

Although the FDA lifted the partial clinical hold after 1 month, on-target, off-tumor toxicity should be considered when developing B7-H3-targeted therapeutics. More recently, we and others have found that B7-H3 is highly and homogeneously expressed on some pediatric cancers, such as Ewing sarcoma, rhabdomyosarcoma, Wilms tumor, and neuroblastoma, as well as brain cancers, such as medulloblastoma and glioblastoma. It has also been reported that B7-H3-targeting CAR-T cells mediate significant anti-tumor effects in preclinical models of these cancer types.<sup>12-14</sup>

not identified. Overexpression of B7-H3 has been found in a variety of human cancers, including lung adenocarcinoma, craniopharyngioma, neuroblastoma, glioma, ovarian cancer, pancreatic cancer, and acute myeloid leukemia (AML),<sup>11-16</sup> whereas its expression is absent or low in normal tissues.<sup>15,17,18</sup>

Although the precise role of B7-H3 in immune regulation and cancer genesis remains unclear, there is no doubt that overexpression of B7-H3 constitutes an attractive biomarker and target for multiple cancer immunotherapy approaches.<sup>19</sup> Several B7-H3-directed therapeutic agents have been undertaken in clinical trials.<sup>20,21</sup> Enoblituzumab, an Fc-optimized monoclonal antibody (mAb) against B7-H3, was evaluated in a phase I clinical study in combination with an anti-programmed death 1 (PD-1) mAb in patients with B7-H3-expressing solid tumors (ClinicalTrials.gov: NCT02475213). Radiolabeled 8H9, another B7-H3-targeting antibody, has also been evaluated in a phase I trial for the treatment of brain and central nervous system tumors, neuroblastoma, and carcinoma (ClinicalTrials.gov: NCT00089245). Notably, last year, the FDA placed a partial hold on two clinical studies of MGD009, a bispecific antibody targeting B7-H3 and CD3

The aims of the present study were the following: (1) to evaluate whether B7-H3 is a high-value target for CAR-T treatment of other cancer types in addition to pediatric tumors and brain cancers and (2) to develop a novel, B7-H3-specific CAR and evaluate its anti-tumor effects in preclinical cancer models.

## RESULTS

### Analysis of B7-H3 Expression in The Cancer Genome Atlas (TCGA) Database

The mRNA expression levels of *CD276* were analyzed using the Gene Expression Profiling Interactive Analysis (GEPIA) web server. Our analysis included the RNA sequencing expression data for 9,433 tumors and 5,540 normal samples from TCGA and the Genotype-Tissue Expression (GTEx) projects. As shown in Figure S1, compared with the expression in normal tissues, B7-H3 expression was significantly higher in 15 of 31 tumor types; ten of the 15 tumor types with B7-H3 overexpression were selected, and their details are shown in Figure 1A. The correlation between B7-H3 expression and survival was also calculated using TCGA datasets. As a result, higher B7-H3 expression predicted a shorter life expectancy in patients with low-grade glioma (LGG)

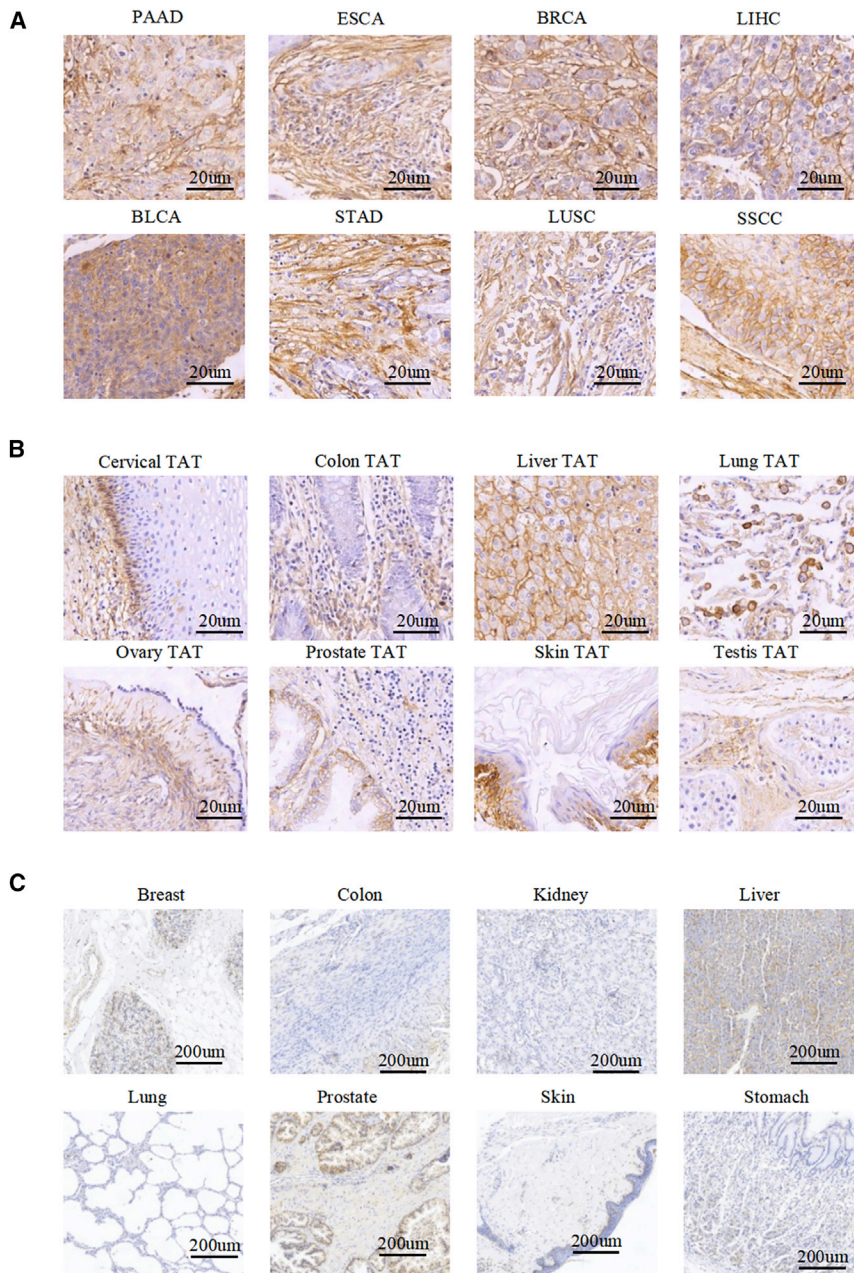


**Figure 2. IHC of B7-H3 in Tumors, TATs, and Normal Tissues**

(A) Microarrays of human tumors were stained for IHC to detect the expression of B7-H3. Representative images are shown, including PAAD, ESCA, breast invasive carcinoma (BRCA), liver hepatocellular carcinoma (LIHC), bladder urothelial carcinoma (BLCA), STAD, lung squamous cell carcinoma (LUSC), and skin squamous cell carcinoma (SSCC). Scale bars, 20  $\mu$ m. (B) IHC staining for B7-H3 expression in a variety of TATs. Scale bars, 20  $\mu$ m. (C) IHC staining for B7-H3 expression in normal tissues. Overall staining results and more staining images are provided in [Tables S1, S2, and S3](#); [Figures S3 and S4](#). Scale bars, 200  $\mu$ m.

[S2, and S3](#). B7-H3 was overexpressed across multiple cancer types, including 88% of bladder urothelial carcinoma (BLCA), 60% of breast invasive carcinoma (BRCA), 89% of esophageal carcinoma (ESCA), 63% of stomach adenocarcinoma (STAD), 80% of liver hepatocellular carcinoma (LIHC), 76% of lung adenocarcinoma (LUAD), 80% of skin squamous cell carcinoma (SSCC), and 61% of pancreatic adenocarcinoma (PAAD). Importantly, we found homogeneous overexpression of B7-H3 in only a small percentage of samples of liver cancer, breast cancer, cervical cancer, bladder cancer, and carcinoma, whereas its expression in other cancer types was highly heterogeneous. Representative images are shown in [Figure 2A](#) and [Figure S3](#).

Notably, B7-H3 was detected with moderate or even high expression levels in 84/209 (40%) tumor-adjacent tissues (TATs) for cancers, such as skin, lung, liver, cervical, ovary, and prostate, but the staining was much weaker than that in the tumor tissues ([Table S2](#)). In some TATs, such as lung and colon TATs, B7-H3 stained positively, mainly in stromal cells ([Figure 2B](#)). We also detected the expression of B7-H3 in 173 human normal tissues. B7-H3 expression was absent or weak in normal tissues, and only three (25%) liver samples, one (13%) prostate sample, two (29%) uterus samples, and three (20%) adrenal gland samples had weak to moderate staining ([Table S3](#); [Figures 2C and S4](#)).

#### Generation and Characterization of mAb Against B7-H3

A B7-H3-specific mAb (mAb-J42) was generated using the traditional hybridoma technique. The B7-H3-specific scFv was derived from mAb-J42 and named J42-scFv. The binding of mAb-J42 and J42-scFv-Fc to cell surface-expressed B7-H3 was confirmed by immunofluorescence (IF) staining using HeLa cells that stably express B7-H3-green fluorescent protein (GFP) ([Figure 3A](#)). HeLa cells exhibit

( $p = 0.0084$ ) or colon adenocarcinoma (COAD) ( $p = 0.0082$ ) ([Figure 1B](#)), whereas no significant differences were found in 9 other tumor types with B7-H3 upregulation ([Figure S2](#)).

#### B7-H3 Expression in Multiple Human Tissues

We performed immunohistochemical (IHC) staining to detect B7-H3 expression in tissue microarrays, including tumor, tumor-adjacent, and normal tissues. Of 209 tumor samples, 18% showed strong staining, 21% moderate staining, and 27% low but detectable staining. A complete description of the IHC results is provided in [Tables S1,](#)

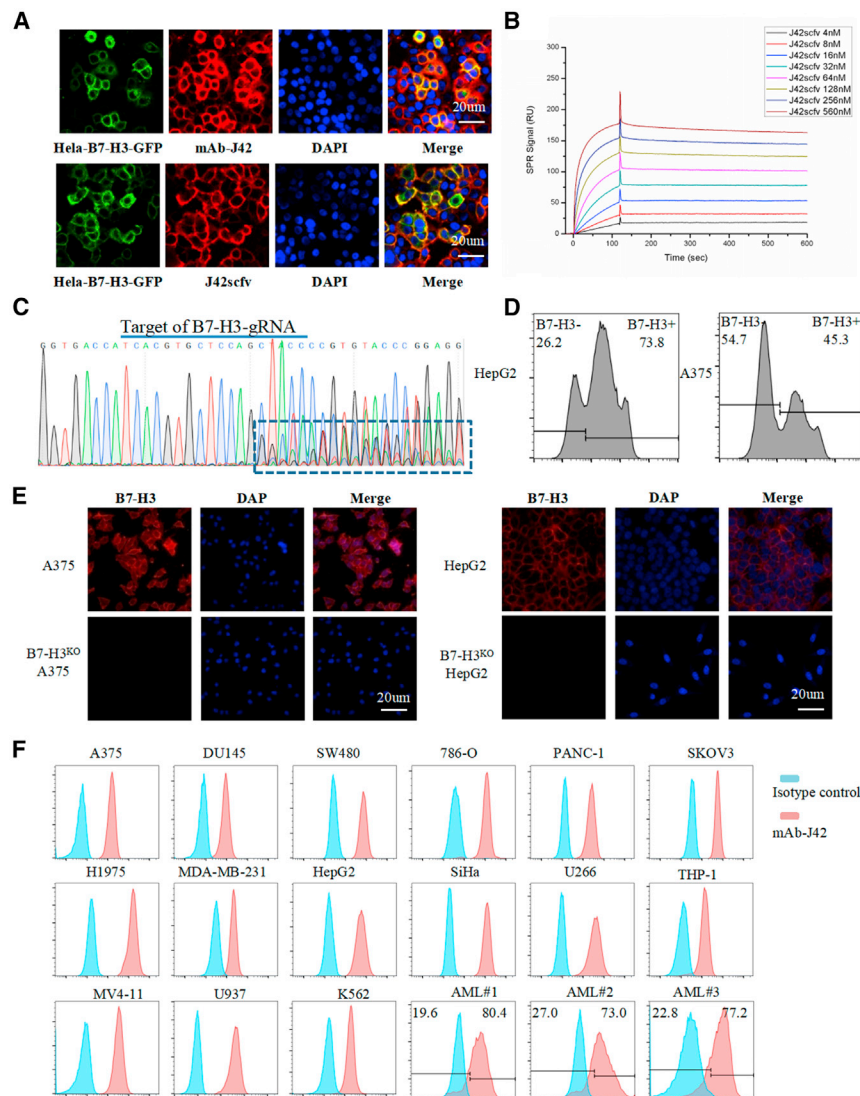


**Figure 3. Generation and Characterization of B7-H3-Specific mAbs and scFv**

(A) Immunofluorescence staining with mAb-J42 and J42-scFv-Fc in HeLa-B7-H3-GFP cells. Cells were incubated with mAb-J42 or J42-scFv-Fc as the primary antibody and then with the Cy3-conjugated secondary antibody. Scale bars, 20  $\mu$ m. (B) The affinity of J42-scFv-Fc binding to B7-H3-ECD-His recombinant protein was determined on a Biacore T100 instrument. (C) Sequencing results for A375 cells, 1 week after transduction with lentivirus carrying B7-H3-targeted gRNA and Cas9. (D) FACS analysis of B7-H3 expression in A375 and HepG2 cells, 1 week after transduction with lentivirus carrying B7-H3-targeted gRNA and Cas9. (E) IF staining with mAb-J42 in FACS-sorted B7-H3<sup>KO</sup> A375 and HepG2 cells and in wild type of A375 and HepG2 cells. Scale bars, 20  $\mu$ m. (F) Expression of B7-H3 in human tumor cell lines and AML patient samples were evaluated by FACS. Cells were incubated with mAb-J42 (red) or its corresponding isotype control (blue).

pirates from patients with monocytic/myelomonocytic AML were obtained and subjected to flow cytometry analysis. As shown in Table S6, the expression of B7-H3 was observed in a median of 57.2% (range 38.8%–80.4%) of primary AML blasts. Representative examples of B7-H3 expression in AML blasts are shown at the bottom of Figure 3F.

**Generation and Characterization of B7-H3-Redirected CAR-T Cells**

B7-H3-redirected CAR was constructed based on a lentiviral vector encoding the B7-H3 binder J42-scFv, CD28 and 4-1BB costimulatory domains, and the CD3- $\zeta$  signaling domain (Figure 4A). mCherry was inserted as a tracker for detecting the expression of CAR with FACS (phycoerythrin [PE]-Texas Red staining in Figure 4B). For the

innate expression of B7-H3 protein. The binding affinity of J42-scFv-Fc to B7-H3 extracellular domain (ECD) recombinant protein was measured using the Biacore X100 instrument (Figure 3B; Table S4). Specific recognition was examined further in knockout of B7-H3 (B7-H3<sup>KO</sup>) cells. Figure 3C shows the sequencing results for A375 cells, 5 days after Cas9/guide RNA (gRNA) transfection and puromycin selection. The binding of J42-scFv-Fc to B7-H3 was analyzed using a fluorescence-activated cell sorter (FACS) (Figure 3D) and IF staining (Figure 3E) in B7-H3<sup>KO</sup> A375 and HepG2 cells.

**B7-H3 Expression in Tumor Cell Lines and AML Clinical Samples**

The expression of B7-H3 in a variety of human tumor cell lines and AML clinical samples was examined by FACS using mAb-J42 as the primary antibody (Figure 3F; Tables S5 and S6). All ten of the solid tumor-derived cell lines and six of the ten hematologic cancer cell lines were positive for B7-H3 (Table S5). Eight bone marrow as-

surance of quality and efficacy of the final CAR-T cells, the phenotype of CAR-T cells was analyzed by FACS, 10 days after lentivirus transduction (Figures 4C and 4D). CAR-T cells were uniformly positive for CD4 and CD8 with a ratio of 1:2. Other markers of T cells, including the central memory T cell markers (CD45RO, CD62 ligand [CD62L]), effector T cell markers (CD25, CD69), and T cell exhaustion markers (PD-1, T cell immunoglobulin [Ig] and mucin domain containing protein-3 [TIM3]), were also examined. The expression of these markers did not differ significantly between the CAR-T cell and nontransduced (NT) groups.

**Functional Test of B7-H3-Redirected CAR-T Cells In Vitro**

The specific recognition and killing of B7-H3-overexpressing cancer cells by CAR-T cells were evaluated using A375 human melanoma cells and MV4-11 leukemia cells as positive controls and Raji human lymphoma cells and peripheral blood mononuclear cells (PBMCs) as

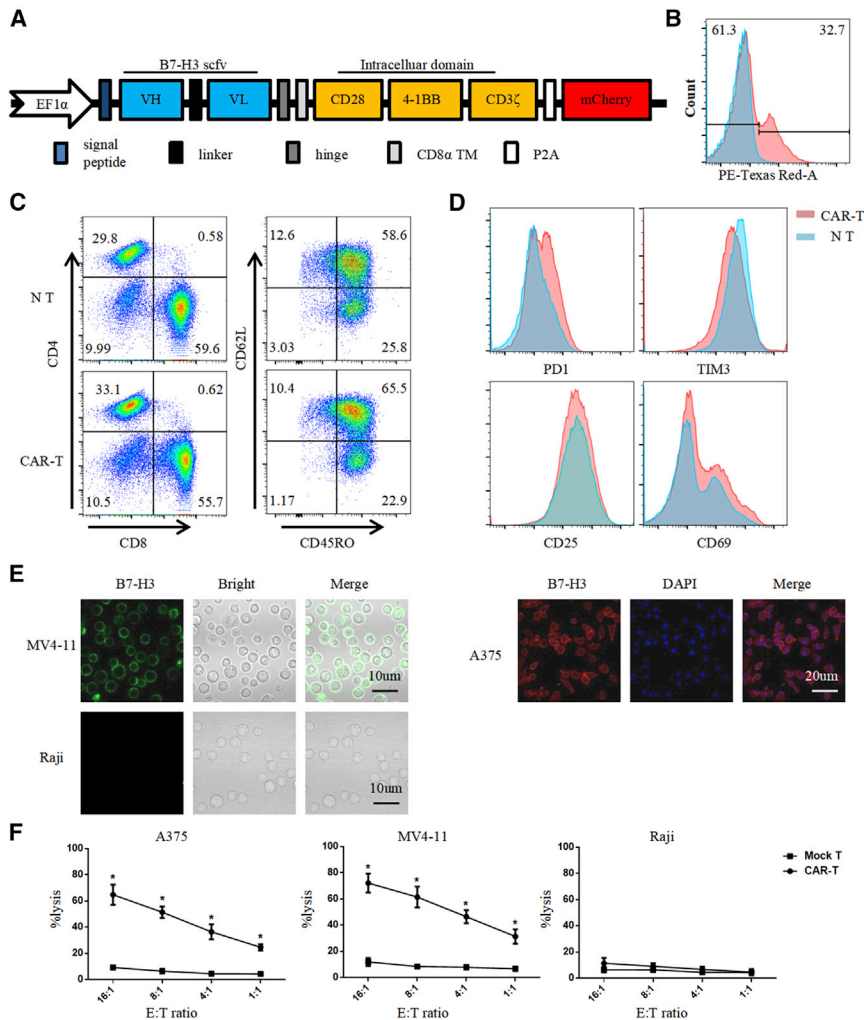


**Figure 4. Production of B7-H3-Redirected CAR-T Cells**

(A) Schematic representation of the B7-H3-targeted CAR construct containing the following fragments: J42-scFv; hinge; CD8 transmembrane domain; intracellular signaling domains of CD28, 4-1BB, and CD3- $\zeta$ ; P2A; and mCherry. (B) B7-H3 CAR expression in human T cells was analyzed by tracking mCherry expression with FACS. (C and D) 10 days after lentivirus CAR transduction, the subsets and phenotype of NT and CAR-T cells were analyzed by FACS, including the expression of (C) CD4, CD8, CD45RO, CD62L and (D) PD1, TIM3, CD25, CD69. (E) Immunofluorescence staining for the expression of B7-H3 (red or green) in A375, MV4-11, and Raji cells. Scale bars, 10  $\mu$ m. (F)  $^{51}$ Cr-release assay to measure the cytotoxicity of CAR-T cells against A375, MV4-11, and Raji cells at different E:T ratios. All error bars represent SD. \* $p < 0.05$ .

AML cells. The percentages of residual tumor cells were estimated from the FACS data, and the results are presented in Figure 5C. Increased secretion of tumor necrosis factor  $\alpha$  (TNF- $\alpha$ ), interleukin (IL)-2, and interferon  $\gamma$  (IFN- $\gamma$ ) was observed in B7-H3-redirected CAR-T cells cocultured with B7-H3-positive tumor cells (A375, MV4-11, HepG2, and U937) but not in cells cocultured with B7-H3-negative Raji cells (Figures 5D–5F).

#### Anti-Tumor Effects of B7-H3-Redirected CAR-T Cells *In Vivo*

To test the efficacy of B7-H3-redirected CAR-T cells against tumors *in vivo*, we adopted two xenograft tumor models of hematological and solid tumors. In the solid tumor model, we injected  $2 \times 10^6$  A375-FFLuc cells subcutaneously into the right flank of NOD-Prkdc<sup>scid</sup>IL2rg<sup>em1</sup>/Smoc (M-NSG) mice. Eight days after tumor inoculation, mice were injected intravenously with a single dose of  $5 \times 10^6$  B7-H3-redirected CAR-T cells, CD19 CAR-T cells, or phosphate-buffered saline (PBS) (Figure 6A). Tumor burden was monitored by *in vivo* bioluminescence imaging (BLI) every 10 day beginning on day 7, and tumor size was measured using a vernier caliper every 3–4 days. As shown in Figures 6B and 6C, B7-H3-redirected CAR-T cells mediated significant regression of xenografts.

In the hematological tumor model, a total of  $2 \times 10^6$  MV411-FFLuc cells were implanted into M-NSG mice via tail-vein injection. Eight days later, when the bioluminescence of the tumors could be detected, mice were infused with  $5 \times 10^6$  B7-H3-redirected CAR-T cells, mock T cells, or PBS via tail-vein injection (Figure 6D). Tumor progression was monitored by BLI every 8 days beginning on day 7 (Figure 6E). Mice in the control group showed rapid progression of leukemia, and most died around 25 days after tumor inoculation. By contrast, almost complete regression of leukemia was observed in mice treated

negative controls. The positive and negative expression of B7-H3 was examined further by IF staining (Figure 4E). The  $^{51}$ Cr-release cytotoxic assay was adopted to test the specific lytic function of B7-H3-redirected CAR-T cells (Figures 4F and S5). B7-H3-redirected CAR-T cells were cocultured with tumor cells for 4 h, after which, CAR-T cells efficiently lysed B7-H3-positive A375 and MV4-11 cells; by contrast, no significant response was observed in B7-H3-negative Raji cells and PBMCs. These cells were cocultured at an effector:target (E:T) ratio of 4:1 for 24 h, and target cell lysis was confirmed by FACS and enzyme-linked immunosorbent assay (ELISA). Representative FACS plots are shown in Figure 5A. A375, Raji, and MV4-11 cells were identified by their B7-H3 expression. The expression of B7-H3 in PBMCs and the cytotoxicity of CAR-T cells against PBMCs were shown in Figure S5.

The secretion of perforin by T cells was also analyzed with FACS (Figure 5B). B7-H3-redirected CAR-T cells mediated tumor cell killing, and perforin secretion increased in B7-H3-positive cells but not in B7-H3-negative cells. CAR-T cells caused 95% cell death in MV4-11

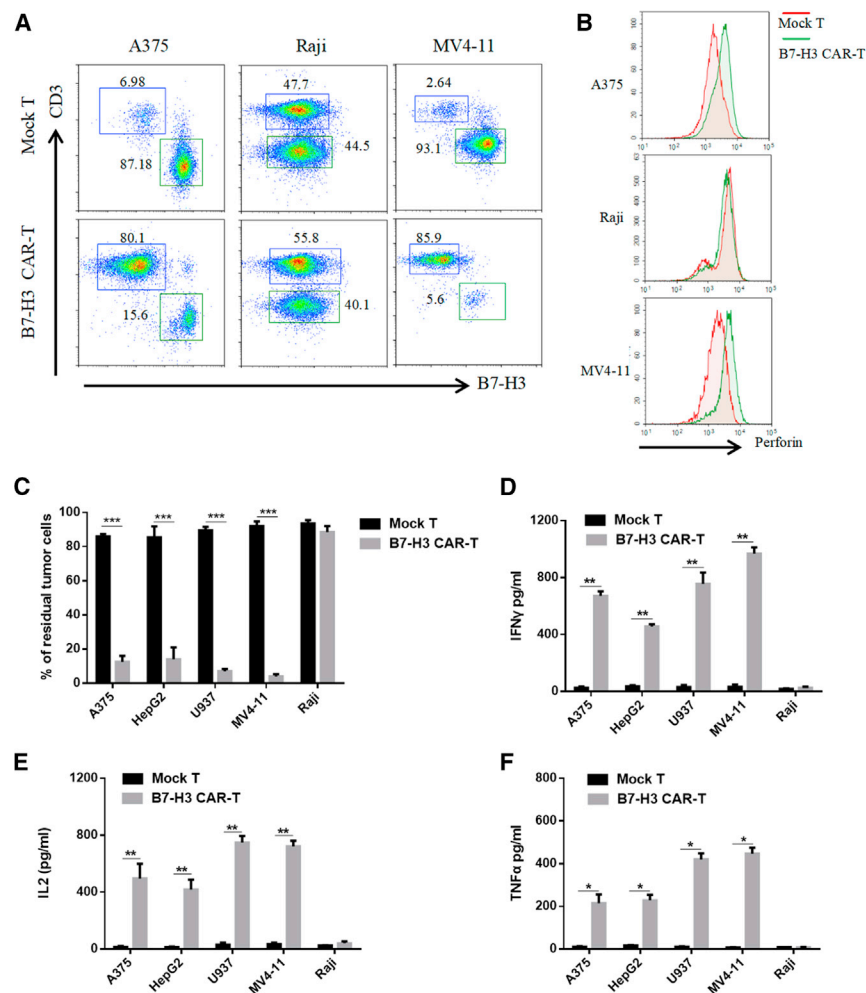


**Figure 5. Anti-Tumor Activity of B7-H3 CAR-T Cells *In Vitro***

(A) Representative flow cytometry plots of mock or CAR-T cells cocultured with tumor cell lines at an E:T ratio of 4:1 for 24 h. A375, Raji, and MV4-11 cells were identified according to their B7-H3 expression. (B) Secretion of perforin from T cells was detected in the same condition as in (A). (C–F) After coculturing mock or CAR-T cells with tumor cells at an E:T ratio of 4:1 for 12 h, the percentages of residual tumor cells were estimated from the FACS data (C), and the concentrations of IFN-γ (D), IL-2 (E), and TNF-α (F) in supernatants were measured by ELISA kits (D–F). All error bars represent SD. \* $p < 0.05$ , \*\* $p < 0.01$ , \*\*\* $p < 0.001$ , one-way ANOVA with Holm–Sidak adjusted  $p$  values.

Therefore, identification of truly tumor-specific target antigens with homogeneous overexpression is the key for treating solid tumors with engineered T cells.

Recently, B7-H3 has emerged as an attractive target for immunotherapy, because it is highly expressed across multiple tumor types but exhibits restricted expression in normal tissues.<sup>13–15</sup> In this study, we performed large-scale screening of the expression of B7-H3 using TCGA data and IHC. We found homogeneous overexpression of B7-H3 only in a small percentage of samples of liver, breast, cervical, and bladder cancers and SSCC, whereas its expression in other cancer types was highly heterogeneous. Notably, the mRNA expression of B7-H3 was ubiquitous in almost all of the normal TATs from TCGA database. In IHC,

with B7-H3-redirection CAR-T cells, as evidenced by BLI. This led to a significant survival advantage compared with mice in the other two groups (Figure 6F). We also examined the B7-H3-positive leukemia cells in peripheral blood using FACS, 15 days after tumor inoculation. Consistent with the BLI results, mice treated with B7-H3-redirection CAR-T cells exhibited significantly decreased tumor burden compared with mock T- or PBS-treated mice (Figure 6G).

## DISCUSSION

Unprecedented success has been achieved in B cell malignancies treated by the adoptive transfer of T cells redirected with a CAR specific for CD19. However, in solid tumors, most of the reported tumor markers are often heterogeneous within tumors, and these markers are expressed in some normal tissues, which lead to limited therapeutic effects or life-threatening toxicity. Epidermal growth factor receptor (EGFR)vIII, a mutant EGFR, is a tumor-specific marker for glioblastoma, but its heterogeneous expression limits the therapeutic efficacy of EGFRvIII CAR-T cells.<sup>22</sup> Treatment with CAR-T cells targeting HER2 caused a patient death because of the recognition of low levels of HER2 on lung epithelial cells.<sup>5</sup>

B7-H3 expression was absent or weak in normal tissues but could be detected at a moderate or even high expression level in some TATs, such as those associated with skin, lung, liver, cervical, ovary, and prostate cancers. Previous work has shown that B7-H3 expression can be induced in normal tissue in response to inflammation.<sup>8</sup> Thus, it will be important in the future to explore its upregulation mechanisms in TATs and to develop more efficient and safer targeted therapy.

A previous study has shown that B7-H3-targeted CAR-T cells have limited activity against K562 cells, a xenograft erythromyeloid leukemia line, because of the lower B7-H3 antigen density on the K562 cell membrane.<sup>14</sup> We examined several cell lines of hematological malignancies and found that MV4-11, an AML cell line, had the highest expression level of B7-H3. With the use of MV4-11 as a model, we found that B7-H3-targeted CAR-T cells displayed significant anti-tumor activity *in vitro* and *in vivo* and caused regression of established cancer and prolonged survival in xenograft tumor models. These findings suggest that the target antigen density is also a key factor for recognition and killing by CAR-T cells.

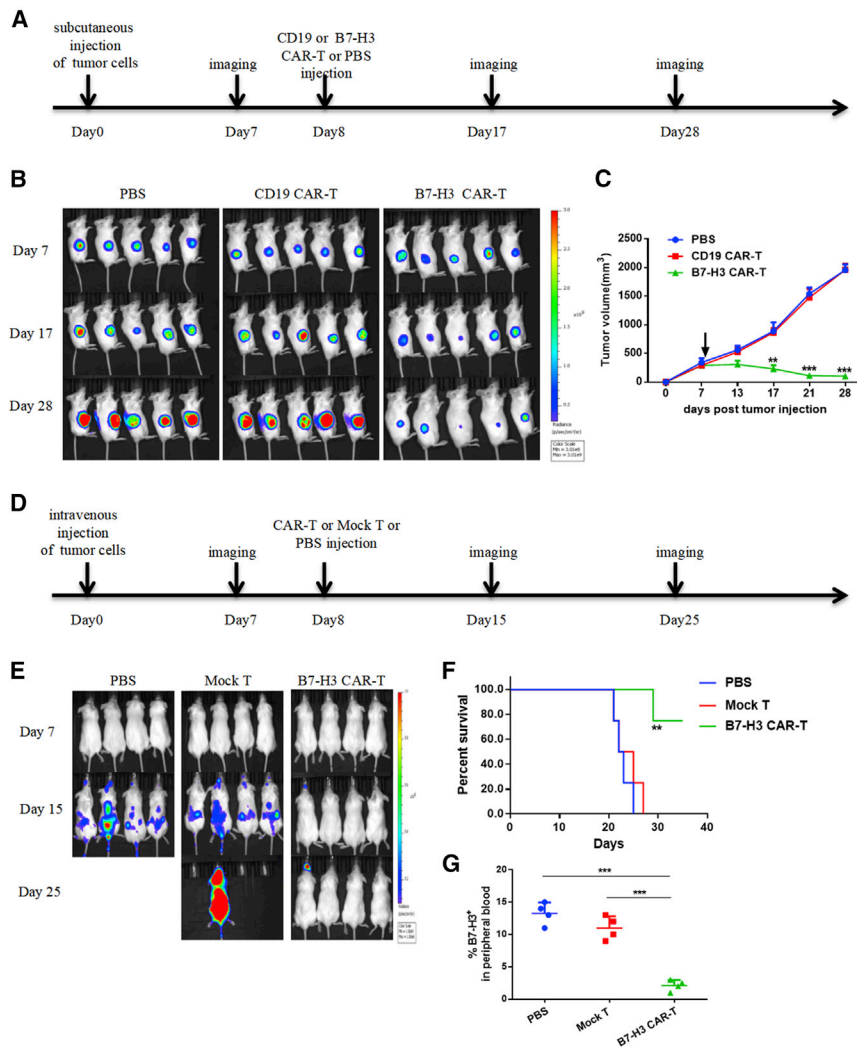


**Figure 6. Anti-Tumor Effects of B7-H3 CAR-T Cells in Xenograft Models**

(A) Treatment scheme used in the A375-FFLuc xenograft model. (B) On days 7, 17, and 28 after tumor injection, an IVIS imaging system was used to monitor tumor growth (five mice per group). (C) Starting on day 7, tumor size was measured using a digital caliper every 3–4 days. The mean values for each treatment group are shown. (D) Treatment scheme used in the MV4-11-FFLuc xenograft model. (E) Tumor progression was monitored by BLI every 8 days beginning on day 7. (F) Overall survival of mice in each group. (G) B7-H3-positive MV4-11 cells in peripheral blood were detected using flow cytometry on day 15 after tumor inoculation. All error bars represent SD. \* $p < 0.05$ , \*\* $p < 0.01$ , \*\*\* $p < 0.001$ .

sion status in surgical specimens before starting targeted therapy. On the other hand, to address the issue of antigenic heterogeneity, the use of bispecific CAR, such as CD19/CD22-bispecific CAR-T cells, has been proposed for the treatment of acute lymphoblastic leukemia (ClinicalTrials.gov: NCT03919526) to overcome the risk of antigen-escape relapse and to improve the duration of the clinical benefit. Thus, the combination of B7-H3 with another tumor antigen in the CAR design may be necessary.

## METHODS

### Mice

6- to 8-week-old immunodeficient M-NSG female mice were purchased from the Model Animal Resource Information Platform of Nanjing University (China). Mice were maintained under specific pathogen-free conditions, and all procedures met the requirements of the National Institutes of Health and Institutional

Animal Care and Use Committee. The animal experiments were approved by the West China Hospital of Sichuan University Biomedical Ethics Committee (ethical approval document: 2018-061).

### Human Tissue Microarray and Clinical Specimens

IHC was performed using human tissue microarrays purchased from Xi'an Alenabio and Shanghai Outdo Biotech of China. Bone marrow aspirates from patients with monocytic/myelomonocytic AML were obtained and subjected to flow cytometry analysis. This study was approved by the West China Hospital of Sichuan University Biomedical Ethics Committee (ethical approval document: 2018-061), and the participating patients provided written, informed consent.

### Cell Lines and Culture Conditions

All tumor cell lines used in this study were originally purchased from the American Type Culture Collection (ATCC). A375-FFLuc and MV4-11-FFLuc cell lines were produced by transducing a lentiviral

Recently, two posters from the American Society of Hematology Annual Meeting reported that B7-H3 is highly expressed in a substantial fraction of AML patients and that adoptive transfer of B7-H3-targeted CARs may be an effective treatment option for AML patients with B7-H3 overexpression. The authors of these posters also reported variable expression patterns of B7-H3 in patients with AML and suggested that it may be necessary to develop a dual-targeting approach, such as combining B7-H3 with a second AML surface antigen.<sup>23,24</sup>

In the present study, using IHC, we observed wide regional variation of B7-H3 expression within and across the tumor tissues. B7-H3 was previously suggested to be a valuable CAR-T target for pancreatic ductal adenocarcinoma, ovarian cancer, and myelogenous leukemia.<sup>14</sup> Here, we also observed positive B7-H3 staining in pancreatic ductal adenocarcinoma and ovarian cancer, but the expression was highly heterogeneous. Antigen heterogeneity is one of the main reasons for failure of CAR-T cell therapy.<sup>5</sup> It may be necessary to examine the B7-H3 expres-

vector that encoded the luciferase reporter gene into the original cell lines. All cells were maintained in Dulbecco's modified Eagle's medium or RPMI-1640 (both from Gibco), supplemented with 10% fetal bovine serum and 2 mM L-glutamine (Invitrogen).

#### Expression of B7-H3 in Tumors from TCGA Database

The expression of B7-H3 in 9,433 tumors and 5,540 normal samples from TCGA database and the GTEx project, including 31 different tumor subtypes, was analyzed using the online web server GEPIA (<http://gepia.cancer-pku.cn>). Data were downloaded, filtered for primary tumors, log<sub>2</sub> transformed, and analyzed using R.

#### Immunohistochemistry

Tissue samples were stained for B7-H3 using a commercial mAb (clone D9M2L; Cell Signaling Technology). All procedures followed the manufacturer's protocol. In brief, tissue sections were incubated at 65°C for 1 h to retrieve antigenicity, blocked with PBS containing 10% normal goat serum (Boster) for 30 min at room temperature, and then incubated with primary antibody at 4°C overnight. The sections were then incubated with goat anti-rabbit secondary antibodies, and the staining was detected with 3,3'-diaminobenzidine (ZSGB-Bio). The staining intensity was scored using a common four-point scale as follows: no expression (-), <20% positive cells (+, low or weak expression), 20%–50% positive cells (++ , moderate expression), and >50% positive cells (+++ , high or strong expression).

#### Lentivirus Production

HEK293FT cells were transfected with the target plasmid and two packaging plasmids pSPAX2 and pMD.2G at a ratio of 4:3:2 using polyethylenimine (Sigma). The supernatants were collected at 48 h and 72 h after transfection, filtered with 0.45 µm filters, and concentrated by ultracentrifugation at 15,000 rpm for 2 h. The concentrated lentivirus was resuspended in RPMI-1640 and immediately stored at -80°C for further use.

#### Overexpression of B7-H3 in HeLa Cells

Full-length human B7-H3 (GenBank: NM\_001024736) was synthesized by Genewiz and cloned into a lentiviral vector with a GFP tag at the C terminus. HeLa cells were transduced with lentiviral vectors, as described above, and selected using puromycin to generate HeLa-B7-H3-GFP cells.

#### Generation of Monoclonal Antibody

The ECD of B7-H3 was subcloned into a eukaryotic expression vector with Fc and His tags at the C terminus. B7-H3-ECD-Fc fusion protein was produced by transiently transfecting HEK293F cells and purified using protein A and nickel-nitrilotriacetic acid (Ni-NTA) affinity columns, and 8- to 10-week-old female BALB/c mice were immunized with B7-H3-ECD-Fc recombinant protein. Hybridomas were produced by fusion of spleen cells with SP2/0 cells. Hybridomas were screened using an ELISA, IF, and flow cytometry.

#### KO of B7-H3 in Tumor Cells

A375 and HepG2 cell lines with B7-H3 KO were produced using a CRISPR-Cas9 system. gRNAs were designed using the online server CHOPCHOP (<http://chopchop.cbu.uib.no>). gRNAs were subcloned into lentiCRISPR version (v.)2 (Addgene; #52961). Lentiviral particles were transduced into A375 and HepG2 cells and selected with puromycin. 1 week after transduction, the cells were stained with mAb-J42, and B7-H3-negative cells were sorted using a FACS (BD Biosciences).

#### Affinity Determinations Using a Biacore Instrument

The binding affinity of mAb-J42 and J42-scFv-Fc to B7-H3 recombinant protein was measured using a Biacore X100 instrument with a CM5 sensor chip (GE Healthcare), according to a previously published procedure.<sup>25</sup> Briefly, B7-H3-ECD-His recombinant protein containing the ECD of B7-H3 with a His tag at the C terminus was produced by transiently transfecting HEK293F cells and purified using Ni-NTA affinity columns and size-exclusion chromatography. Fc-tagged J42-scFv was expressed, as mentioned above, for B7-H3-ECD-Fc protein. A rabbit anti-mouse IgG antibody (mouse antibody capture kit; GE Healthcare) was immobilized on CM5 using amine coupling (amine coupling kit; GE Healthcare), mAb-J42 and Fc-tagged J42-scFv were indirectly captured onto the surface, and the B7-H3-ECD-His protein was injected across the chip in a 2-fold dilution series. The equilibrium dissociation constant was obtained by using BIAevaluation 2.0 software.

#### Immunofluorescence Staining

Cells were incubated in 24-well plates under standard cell-culture conditions. After 24 h, the cells were blocked with 1% bovine serum albumin for 30 min, stained with primary antibody (mAb-J42 or J42-scFv-Fc) for 1 h at 4°C, fixed in 4% paraformaldehyde for 15 min, and stained with fluorescein isothiocyanate (FITC)- or Cy3-conjugated secondary antibody (Proteintech) and 4',6-diamidino-2-phenylindole (Beyotime). Images were captured on a confocal microscope (Zeiss 880).

#### Flow Cytometry and Antibodies

B7-H3 expression levels on the surface of human tumor cells were detected using purified mAb-J42 or J42-scFv-Fc. Goat anti-mouse IgG-FITC (Proteintech) was used to label the Fc of mAb-J42. The antibodies used to identify the phenotype of CAR-T cells included CD3-allophycocyanin (APC)-CY7, perforin-APC, CD4-PE, CD8-FITC, TIM3-BV711, and PD-1-BV605 (all purchased from BioLegend). Flow cytometry analysis was performed on a BD Fortessa flow cytometer and analyzed using FlowJo 10.6.0 software.

#### T Cell Transduction

The B7-H3-specific binder J42-scFv was derived from mAb-J42 by coconnection of the variable heavy (VH) and variable light (VL) with a G4S linker. B7-H3-redirected CAR was constructed using a lentiviral vector encoding J42-scFv, CD28 and 4-1BB costimulatory domains, and the CD3-ζ-signaling domain, with the human eukaryotic translation elongation factor 1 alpha (EF1α) as the promoter.



Human peripheral blood mononuclear cells from healthy donors were isolated using density gradient centrifugation and activated by culturing with anti-CD3 mAb (OKT3, 100 ng/mL; BioLegend), CD28 mAb (CD28.2, 100 ng/mL; BioLegend), and recombinant human IL-2 (100 units/mL; Life Science) in X-vivo medium (Lonza), supplemented with 2 mM L-glutamine, 10 mM HEPES, 100 U/mL penicillin, and 100 µg/mL streptomycin. On day 2, activated T cells were transduced with lentivirus particles using hexadimethrine bromide (polybrene) (Sigma) for 12 h and then cultured continuously for 10–14 days. Mock T cells and CD19 CAR-T cells were established under the same conditions, and NT cells were not transduced with lentivirus.

### Cytotoxicity Assays

The  $^{51}\text{Cr}$  assay was adopted to detect the cytotoxicity of B7-H3-redirected CAR-T cells, as previously described.<sup>26</sup> Briefly, CAR-T cells and tumor cells were labeled with sodium chromate (molecular formula:  $\text{Na}_2^{51}\text{CrO}_4$ ) and cocultured at an E:T ratio of 16:1, 8:1, 4:1, and 1:1 for 4 h. The supernatants were collected, and the radioactivity was measured using a gamma counter. The percentage of specific lysis was calculated by the following formula:  $(\text{test release} - \text{spontaneous release}) / (\text{maximal release} - \text{spontaneous release}) \times 100$ .

### T Cell Functional Assays

B7-H3-redirected CAR-T cells ( $4 \times 10^5$ ) and tumor cells ( $1 \times 10^5$ ) were cocultured in 24-well plates at 37°C without addition of exogenous cytokines. After 24 h, the cells were harvested for flow cytometry analysis. Residual tumor cells and perforin secretion by CAR-T cells were measured by flow cytometry. For ELISA assays, CAR-T cells and tumor cells were cocultured at an E:T ratio of 4:1 at 37°C, without the addition of exogenous cytokines for 12 h, and the supernatant was collected from each coculture. The concentrations of IL-2, TNF- $\alpha$ , and IFN- $\gamma$  in the supernatant were measured using ELISA kits (BioLegend).

### Tumor Models and Treatment

In the solid tumor model, each mouse was injected subcutaneously in the right flank with  $2 \times 10^6$  A375-FFLuc. On day 7, the mice were randomly divided into three groups, five mice per group. On day 8, the mice were injected intravenously with  $5 \times 10^6$  B7-H3 CAR-T cells in 200 µL, an equal number of CD19 CAR-T cells, or an equal volume of PBS, respectively. The progress of tumor growth was monitored by measuring the bioluminescence signal and size using a vernier caliper. The tumor volume was calculated as follows:  $\text{tumor size} = \text{long diameter} \times (\text{short diameter}^2) / 2$ .

In the hematologic tumor model,  $2 \times 10^6$  MV4-11-FFLuc leukemia cells were injected into the tail vein. 7 days later, mice were divided into three groups and treated with PBS,  $1 \times 10^7$  mock T cells, or  $1 \times 10^7$  B7-H3 CAR-T cells, respectively. To monitor tumor growth, the In Vivo Imaging System (IVIS) (Caliper Life Sciences) was used to record mice bioluminescence imaging. Bioluminescence was activated 10 min after intraperitoneal injection with 150 mg/kg D-luciferin (Beyotime). Living Image software (PerkinElmer) was used to analyze the data.

erin (Beyotime). Living Image software (PerkinElmer) was used to analyze the data.

### Data Visualization and Statistical Analysis

The data were visualized on graphs and are presented as mean  $\pm$  standard deviation (SD). The data were analyzed using GraphPad Prism software v.7.0. For Kaplan–Meier overall survival analysis, a log-rank test was used to compare each of the arms. Student's t test was used to compare the degree of killing by CAR-T cells and mock T cell products. Tumor growth data were analyzed using two-way analysis of variance (ANOVA). Differences between the means for the numbers of B7-H3-positive leukemia cells in peripheral blood were assessed using one-way ANOVA with Bonferroni's post-test correction.  $p < 0.05$  was considered to be significant, and the significance levels are represented in the figures as \* $p < 0.05$ , \*\* $p < 0.01$ , and \*\*\* $p < 0.001$ .

### Ethics Approval and Consent to Participate

The project protocol was approved by the Biomedical Ethics Committee of West China Hospital of Sichuan University. The use of primary tumor samples obtained from patients and blood samples from patients or donors was approved by the West China Hospital of Sichuan University Biomedical Ethics Committee (ethical approval document 2018-061). Written, informed consent was obtained from patients and donors.

### SUPPLEMENTAL INFORMATION

Supplemental Information can be found online at <https://doi.org/10.1016/j.omto.2020.03.019>.

### AUTHOR CONTRIBUTIONS

Z.Z., C.J., and Z.L. performed the experiments, analyzed the data, and wrote the manuscript. C.J., Z.Z., and M.T. performed the hybridoma screening and antibody generation. X.T., Y.W., J.H., M.Y., M.T., and M.Z. participated in the vector construction, sample collection, and animal experiments. K.Z., S.Z., and M.T. participated in the protein purification, CAR-T cell manufacture, and data collection. T.Z. performed the bioinformatics analysis. H.Y., G.G., and L.Z. participated in the design of the experimental work, provided expertise for IHC, and critically reviewed the manuscript. J.X. and A.T. conceived the study, designed the experiments, supervised the research, and wrote the manuscript. All authors read and approved the final manuscript.

### CONFLICTS OF INTEREST

C.J., Z.Z., and A.T. have filed patents related to this work. The other authors declare no competing interests.

### ACKNOWLEDGMENTS

The authors have obtained consent to publish from the participants to report individual patient data. All authors agree to submit the manuscript for consideration for publication. This work was supported by the National Natural Science Foundation of China (31471286), National Major Scientific and Technological Special Project for Significant New Drugs Development (2019ZX09301-147), 1.3.5 Project for Disciplines of Excellence of the West China Hospital, Sichuan

University (ZYJC18007), and Major Subject of the Science and Technology Department of Sichuan Province (2017SZ0015 and 2019YFS0108).

## REFERENCES

- Rosenberg, S.A., and Restifo, N.P. (2015). Adoptive cell transfer as personalized immunotherapy for human cancer. *Science* *348*, 62–68.
- Sadelain, M., Brentjens, R., and Rivière, I. (2013). The basic principles of chimeric antigen receptor design. *Cancer Discov.* *3*, 388–398.
- Johnson, L.A., and June, C.H. (2017). Driving gene-engineered T cell immunotherapy of cancer. *Cell Res.* *27*, 38–58.
- Mirzaei, H.R., Rodriguez, A., Shepphird, J., Brown, C.E., and Badie, B. (2019). Corrigendum: Chimeric Antigen Receptors T Cell Therapy in Solid Tumor: Challenges and Clinical Applications. *Front. Immunol.* *10*, 780.
- Morgan, R.A., Yang, J.C., Kitano, M., Dudley, M.E., Laurencot, C.M., and Rosenberg, S.A. (2010). Case report of a serious adverse event following the administration of T cells transduced with a chimeric antigen receptor recognizing ERBB2. *Mol. Ther.* *18*, 843–851.
- Prasad, D.V.R., Nguyen, T., Li, Z., Yang, Y., Duong, J., Wang, Y., and Dong, C. (2004). Murine B7-H3 is a negative regulator of T cells. *J. Immunol.* *173*, 2500–2506.
- Chapoval, A.I., Ni, J., Lau, J.S., Wilcox, R.A., Flies, D.B., Liu, D., Dong, H., Sica, G.L., Zhu, G., Tamada, K., and Chen, L. (2001). B7-H3: a costimulatory molecule for T cell activation and IFN-gamma production. *Nat. Immunol.* *2*, 269–274.
- Veenstra, R.G., Flynn, R., Kreymborg, K., McDonald-Hyman, C., Saha, A., Taylor, P.A., Osborn, M.J., Panoskaltis-Mortari, A., Schmitt-Graeff, A., Lieberknecht, E., et al. (2015). B7-H3 expression in donor T cells and host cells negatively regulates acute graft-versus-host disease lethality. *Blood* *125*, 3335–3346.
- Steinberger, P., Majdic, O., Derdak, S.V., Pfistershammer, K., Kirchberger, S., Klauser, C., Zlabinger, G., Pickl, W.F., Stöckl, J., and Knapp, W. (2004). Molecular characterization of human 4Ig-B7-H3, a member of the B7 family with four Ig-like domains. *J. Immunol.* *172*, 2352–2359.
- Suh, W.K., Gajewska, B.U., Okada, H., Gronski, M.A., Bertram, E.M., Dawicki, W., Duncan, G.S., Bukczynski, J., Plyte, S., Elia, A., et al. (2003). The B7 family member B7-H3 preferentially down-regulates T helper type 1-mediated immune responses. *Nat. Immunol.* *4*, 899–906.
- Tang, X., Zhao, S., Zhang, Y., Wang, Y., Zhang, Z., Yang, M., Zhu, Y., Zhang, G., Guo, G., Tong, A., and Zhou, L. (2019). B7-H3 as a Novel CAR-T Therapeutic Target for Glioblastoma. *Mol. Ther. Oncolytics* *14*, 279–287.
- Nehama, D., Di Ianni, N., Musio, S., Du, H., Patané, M., Pollo, B., Finocchiaro, G., Park, J.J.H., Dunn, D.E., Edwards, D.S., et al. (2019). B7-H3-redirected chimeric antigen receptor T cells target glioblastoma and neurospheres. *EBioMedicine* *47*, 33–43.
- Du, H., Hirabayashi, K., Ahn, S., Kren, N.P., Montgomery, S.A., Wang, X., Tiruthani, K., Mirklekar, B., Michaud, D., Greene, K., et al. (2019). Antitumor Responses in the Absence of Toxicity in Solid Tumors by Targeting B7-H3 via Chimeric Antigen Receptor T Cells. *Cancer Cell* *35*, 221–237.e8.
- Majzner, R.G., Theruvath, J.L., Nellan, A., Heitzeneder, S., Cui, Y., Mount, C.W., Rietberg, S.P., Linde, M.H., Xu, P., Rota, C., et al. (2019). CAR T Cells Targeting B7-H3, a Pan-Cancer Antigen, Demonstrate Potent Preclinical Activity Against Pediatric Solid Tumors and Brain Tumors. *Clin. Cancer Res.* *25*, 2560–2574.
- Seaman, S., Zhu, Z., Saha, S., Zhang, X.M., Yang, M.Y., Hilton, M.B., Morris, K., Szot, C., Morris, H., Swing, D.A., et al. (2017). Eradication of Tumors through Simultaneous Ablation of CD276/B7-H3-Positive Tumor Cells and Tumor Vasculature. *Cancer Cell* *31*, 501–515.e8.
- Guery, T., Roumier, C., Berthon, C., Renneville, A., Preudhomme, C., and Quesnel, B. (2015). B7-H3 protein expression in acute myeloid leukemia. *Cancer Med.* *4*, 1879–1883.
- Hofmeyer, K.A., Ray, A., and Zang, X. (2008). The contrasting role of B7-H3. *Proc. Natl. Acad. Sci. USA* *105*, 10277–10278.
- Inamura, K., Yokouchi, Y., Kobayashi, M., Sakakibara, R., Ninomiya, H., Subat, S., Nagano, H., Nomura, K., Okumura, S., Shibutani, T., and Ishikawa, Y. (2017). Tumor B7-H3 (CD276) expression and smoking history in relation to lung adenocarcinoma prognosis. *Lung Cancer* *103*, 44–51.
- Lee, Y.H., Martin-Orozco, N., Zheng, P., Li, J., Zhang, P., Tan, H., Park, H.J., Jeong, M., Chang, S.H., Kim, B.S., et al. (2017). Inhibition of the B7-H3 immune checkpoint limits tumor growth by enhancing cytotoxic lymphocyte function. *Cell Res.* *27*, 1034–1045.
- Kramer, K., Kushner, B.H., Modak, S., Pandit-Taskar, N., Smith-Jones, P., Zanzonico, P., Humm, J.L., Xu, H., Wolden, S.L., Souweidane, M.M., et al. (2010). Compartmental intrathecal radioimmunotherapy: results for treatment for metastatic CNS neuroblastoma. *J. Neurooncol.* *97*, 409–418.
- Souweidane, M.M., Kramer, K., Pandit-Taskar, N., Zhou, Z., Haque, S., Zanzonico, P., Carrasquillo, J.A., Lyashchenko, S.K., Thakur, S.B., Donzelli, M., et al. (2018). Convection-enhanced delivery for diffuse intrinsic pontine glioma: a single-centre, dose-escalation, phase 1 trial. *Lancet Oncol.* *19*, 1040–1050.
- O'Rourke, D.M., Nasrallah, M.P., Desai, A., Melenhorst, J.J., Mansfield, K., Morrisette, J.J.D., Martinez-Lage, M., Brem, S., Maloney, E., Shen, A., et al. (2017). A single dose of peripherally infused EGFRvIII-directed CAR T cells mediates antigen loss and induces adaptive resistance in patients with recurrent glioblastoma. *Sci. Transl. Med.* *9*, eaaa0984.
- Lichtman, E., Du, H.W., Savoldo, B., Ferrone, S., Li, G.M., Su, L.S., and Dotti, G. (2018). Pre-Clinical Evaluation of B7-H3-Specific Chimeric Antigen Receptor T-Cells for the Treatment of Acute Myeloid Leukemia. *Blood* *132* (Suppl 1), 701, <https://doi.org/10.1182/blood-2018-99-113468>.
- Guéry, T., Roumier, C., Berthon, C., Lepelley, P., Renneville, A., Nibourel, O., Dumezy, F., Soenen, V., Roche, C., Preudhomme, C., and Quesnel, B. (2013). The B7-H3 Protein In Acute Myeloid Leukemia. *Blood* *122*, 2620. V122.21.2620.2620. <https://doi.org/10.1182/blood>.
- Pope, M.E., Soste, M.V., Eyford, B.A., Anderson, N.L., and Pearson, T.W. (2009). Anti-peptide antibody screening: selection of high affinity monoclonal reagents by a refined surface plasmon resonance technique. *J. Immunol. Methods* *341*, 86–96.
- Gottschalk, S., Edwards, O.L., Sili, U., Huls, M.H., Goltsova, T., Davis, A.R., Heslop, H.E., and Rooney, C.M. (2003). Generating CTLs against the subdominant Epstein-Barr virus LMP1 antigen for the adoptive immunotherapy of EBV-associated malignancies. *Blood* *101*, 1905–1912.

OMTO, Volume 17

## **Supplemental Information**

### **B7-H3-Targeted CAR-T Cells**

#### **Exhibit Potent Antitumor Effects**

#### **on Hematologic and Solid Tumors**

**Zongliang Zhang, Caiying Jiang, Zhiyong Liu, Meijia Yang, Xin Tang, Yuelong Wang, Meijun Zheng, Jianhan Huang, Kunhong Zhong, Shasha Zhao, Mei Tang, Tingyue Zhou, Hui Yang, Gang Guo, Liangxue Zhou, Jianguo Xu, and Aiping Tong**

**Table S1. B7-H3 expression patterns in human tumour tissues analysed with IHC**

Tumor Type	#Stained	Positive (%)	Intensity			
			- (%)	+ (%)	++ (%)	+++ (%)
Bladder: BLCA	16	88	12	19	25	44
Breast: BRCA	10	60	40	10	20	30
Cervical: CESC	14	57	43	36	14	7
Colorectal: COAD	16	44	56	12	19	13
Esophageal: ESCA	9	89	11	11	11	67
Stomach: STAD	8	63	37	13	25	25
Kidney: KIRP	10	60	40	10	40	10
Liver: LIHC	15	80	20	13	40	27
Lung: LUSC	21	76	24	18	29	29
Lymphoma: DLBC	7	71	29	42	29	0
Skin: SSCC	20	80	20	15	15	50
Ovarian: OV	11	64	36	27	18	19
Pancreatic: PAAD	23	61	39	17	13	31
Prostate: PRAD	18	50	50	11	6	33
Testis: ANSE and SEMI	5	20	80	20	0	0
Testis: EMCA	4	100	0	50	50	0
Tongue: ERMS	2	0	100	0	0	0
Total tumor tissue:	209	66	34	18	21	27

Note: The expression levels were scored as no expression (-), < 20% positive cells (+, low or weak expression), 20-50% positive cells (++, moderate expression), and > 50% positive cells (+++, high or strong expression).

BLCA: Bladder Urothelial Carcinoma, BRCA: Breast invasive carcinoma, CESC: Cervical squamous cell carcinoma, COAD: Colon adenocarcinoma, ESCA: Esophageal carcinoma, STAD: Stomach adenocarcinoma, KIRC: Kidney renal clear cell carcinoma, LIHC: Liver hepatocellular carcinoma, LUSC: Lung squamous cell carcinoma, DLBC: Diffuse Large B-cell Lymphoma, SSCC: Skin squamous cell carcinoma, OV: Ovarian serous cystadenocarcinoma, PAAD: Pancreatic adenocarcinoma, PRAD: Prostate adenocarcinoma, ANSE: Anaplasia seminoma, SEMI: seminoma, EMCA: Embryonal carcinoma, ERMS: Embryonal rhabdomyosarcoma.

**Table S2. B7-H3 expression patterns in human TATs analysed with IHC**

Tumor Type	#Stained	Positive (%)	Intensity			
			- (%)	+ (%)	++ (%)	+++ (%)
Bladder (TAT)	16	19	81	19	0	0
Breast (TAT)	10	10	90	10	0	0
Cervical (TAT)	14	29	71	29	0	0
Colorectal (TAT)	16	63	38	44	19	0
Esophageal (TAT)	9	33	67	0	33	0
Stomach (TAT)	8	63	38	13	25	0
Kidney (TAT)	10	0	100	0	0	0
Liver (TAT)	15	53	47	27	27	0
Lung (TAT)	21	52	48	29	24	0
Lymphoma (TAT)	7	29	71	14	0	0
Skin (TAT)	20	55	45	25	30	0
Ovarian (TAT)	11	45	55	27	18	0
Pancreatic (TAT)	23	35	65	17	17	0
Prostate (TAT)	18	33	67	22	11	0
Testis (TAT)	9	56	44	56	0	0
Placenta (TAT)	2	100	0	0	100	0
Total TAT:	209	84	125	23	16	0

Note: TAT: tumor adjacent tissues; The expression levels were scored as no expression (-), < 20% positive cells (+, low or weak expression), 20-50% positive cells (++, moderate expression), and > 50% positive cells (+++, high or strong expression).

**Table S3. B7-H3 expression patterns in human normal tissues analysed with IHC**

Tumor Type	#Stained	Positive (%)	Intensity			
			- (%)	+ (%)	++ (%)	+++ (%)
Breast	5	20	80	20	0	0
Cerebellum	8	0	100	0	0	0
Cerebrum	8	13	87	13	0	0
Esophagus	6	17	83	17	0	0
Stomach	6	0	100	0	0	0
Intestine	8	0	100	0	0	0
Colon	4	25	75	25	0	0
Heart	4	0	100	0	0	0
Kidney	8	0	100	0	0	0
Liver	12	67	33	42	25	0
Lung	9	0	100	0	0	0
Ovary	5	60	40	60	0	0
Pancreas	6	17	83	17	0	0
Prostate	8	38	62	25	13	
Skin	10	0	100	0	0	0
Testis	4	50	50	50	0	0
Thyroid	9	0	100	0	0	0
Tonsils	5	20	80	20	0	0
Uterus	7	43	57	14	29	0
Adrenal gland	15	40	60	20	20	0
Spleen	6	0	100	0	0	0
Bladder	8	13	87	13	0	0
Larynx	7	14	86	14	0	0
Salivary gland	5	20	80	20	0	0
Total tumor tissue:	173	20	80	14	6	0

Note: The expression levels were scored as no expression (-), < 20% positive cells (+, low or weak expression), 20-50% positive cells (++, moderate expression), and > 50% positive cells (+++, high or strong expression).

**Table S4. Affinity analysis of mAb-J42 and J42-scFv-Fc with B7-H3-ECD-His**

<b>Antibody</b>	<b>Ka (1/MS)</b>	<b>Kd (1/s)</b>	<b>KD(pM)</b>
mAb-J42	$5.619 \times 10^5$	$3.729 \times 10^{-5}$	66.36
J42-scFv-Fc	$1.957 \times 10^5$	$2.515 \times 10^{-5}$	128.5

Note: The binding affinity was measured using the Biacore<sup>TM</sup> X100 instrument with CM5 sensor chip (GE Healthcare). mAb-J42 and Fc-tagged J42-scFv were indirectly captured onto the surface, and the B7-H3-ECD-His protein was injected across the chip in a twofold dilution series. The equilibrium dissociation constant (KD) was obtained using BIAevaluation 2.0 software.

**Table S5. B7-H3 expression in tumor cell lines**

<b>Cell line</b>	<b>Tumor type</b>	<b>B7-H3</b>	<b>Cell line</b>	<b>Tumor type</b>	<b>B7-H3</b>
A375	melanoma	+	SKOV3	ovarian cancer	+
DU145	prostate cancer	+	H1975	lung cancer	+
SW480	colon cancer	+	MDA-MB-231	breast cancer	+
786-O	renal cancer	+	HepG2	liver cancer	+
PANC-1	pancreatic cancer	+	SiHa	cervical cancer	+
U266	multiple myeloma	+	THP-1	monocytic leukemia	+
MV4-11	B myelomonocytic leukemia	+	U937	histiocytic lymphoma	+
K562	myelogenous leukemia	+	HL-60	promyelocytic leukemia	+
Jurkat	T cell leukemia	-	Raji	Burkitt's lymphoma	-
Daudi	Burkitt's lymphoma	-	Ramos	Burkitt's lymphoma	-

Note: +, positive; -, negative.



**Table S6. Characteristics of AML**

<b>AML Sample ID</b>	<b>Age</b>	<b>Sex</b>	<b>Cytogenetics</b>	<b>B7-H3% positive</b>
1	10 years	male	t(3;11), MLL-R	80.4
2	8 years	male	t(6;11), MLL-R	73.0
3	15 years	female	PML/RARA+	77.2
4	22 years	male	inv(3)(q21.3q26.2)	45.7
5	15 years	male	46, XY	40.5
6	6 years	male	t(4;11), MLL-R	42.1
7	7 years	female	PML/RARA+	38.8
8	31 years	male	46, XY	60.2

Note: Bone marrow aspirates from patients with monocytic/myelomonocytic AML were obtained and subjected to flow cytometry assay.

## Fold Change Between Tumor and Normal

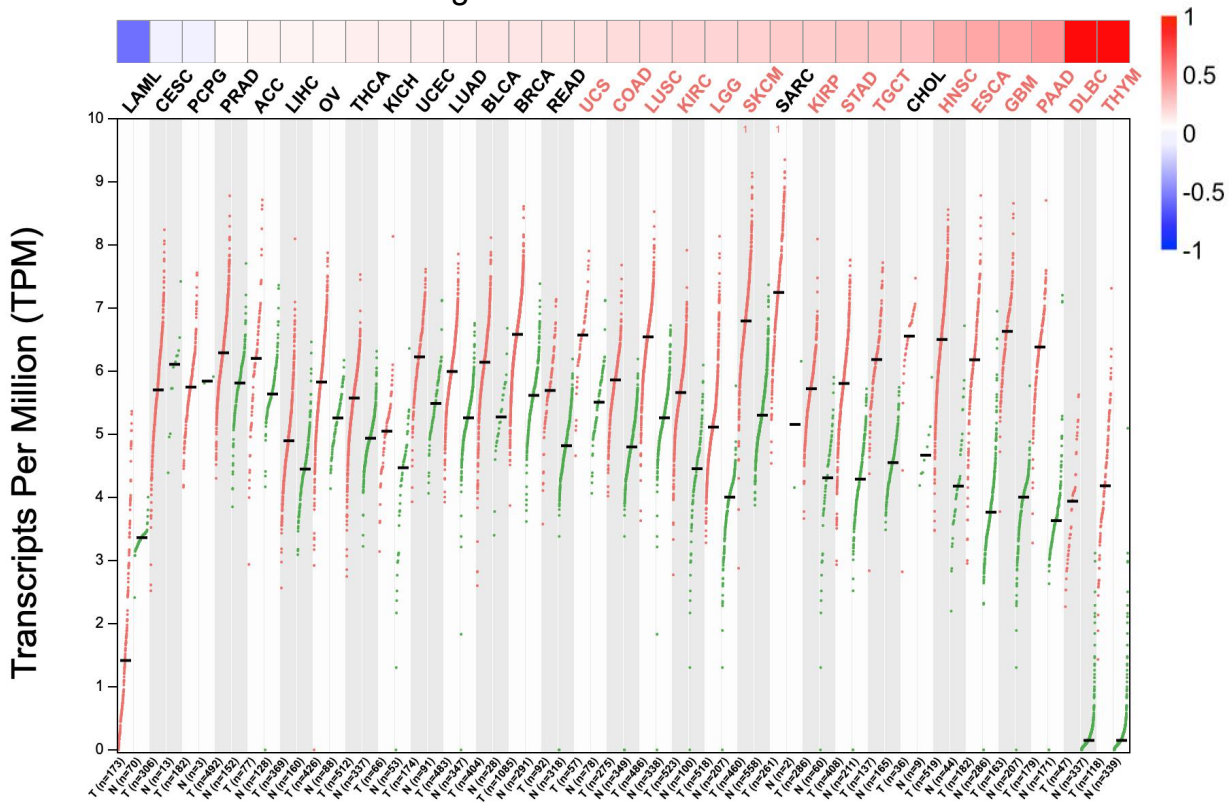


**Figure S1. B7-H3 expression analysis using GEPIA**

Expression level of B7-H3 in 9433 tumor samples and 5540 normal samples from the TCGA and the GTEx projects including 31 tumor subtypes were analyzed using GEPIA web server (<http://gepia.cancer-pku.cn>).

The upper color indicator bar indicates the expression fold changes in tumor samples compared to normal samples.

Tumor subtypes shown in red font represent statistically significant upregulation in tumor samples ( $p < 0.05$ ).

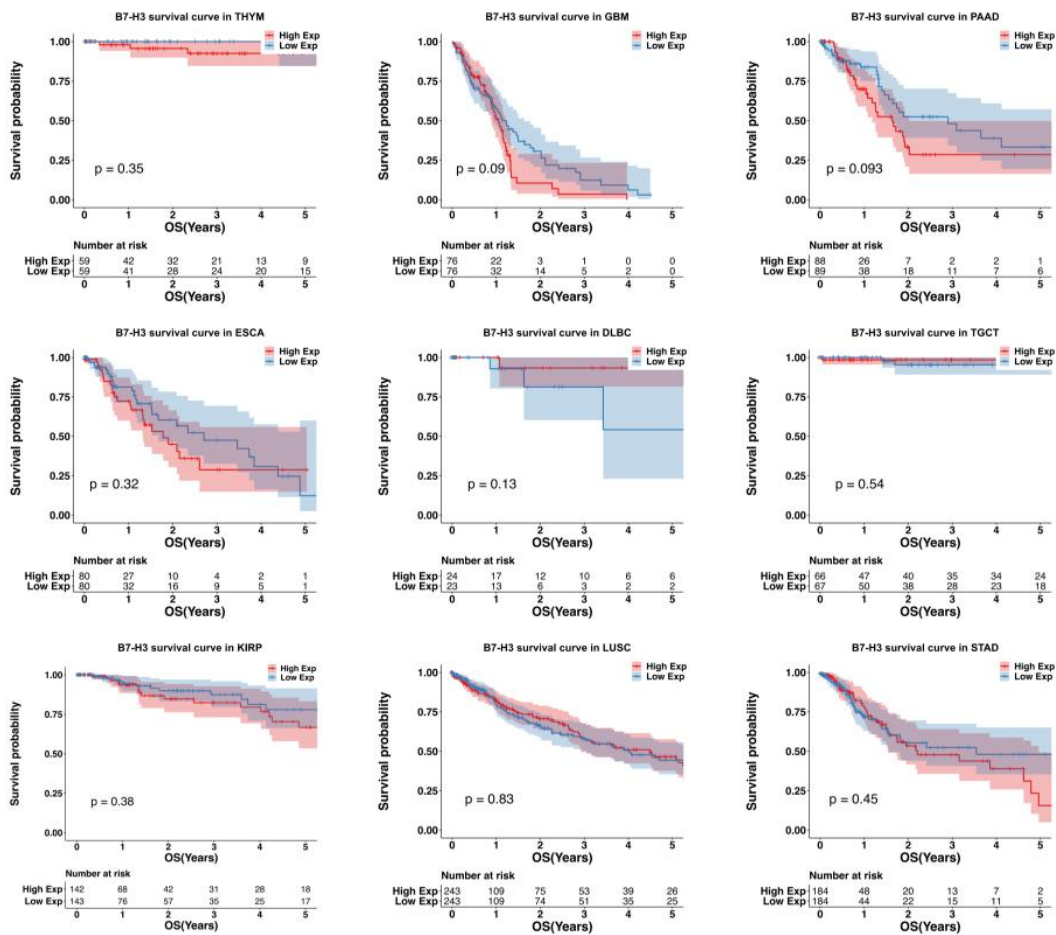


**Figure S2. Correlation analysis between B7-H3 expression and survival using GEPIA**

Correlation analysis between B7-H3 expression and survival across 9 common tumor subtypes (THYM, GBM, PAAD, ESCA, DLBC, TGCT, KIRP, LUSC and STAD) were performed by using GEPIA web server (<http://gepia.cancer-pku.cn>).

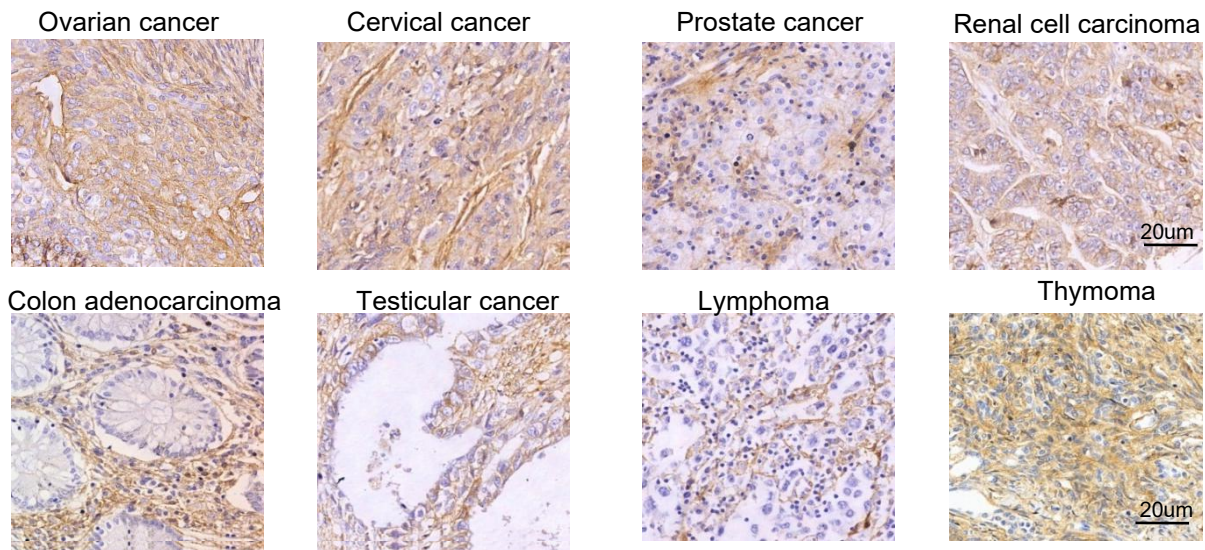


**Figure S3. IHC staining for B7-H3 expression in human tumor tissues**

Representative IHC images of B7-H3 expression in human cancer tissues including ovarian cancer, cervical cancer, prostate cancer, renal cell carcinoma, colon adenocarcinoma, testicular cancer, lymphoma and thymoma.

Scale bars, 20  $\mu$ m.

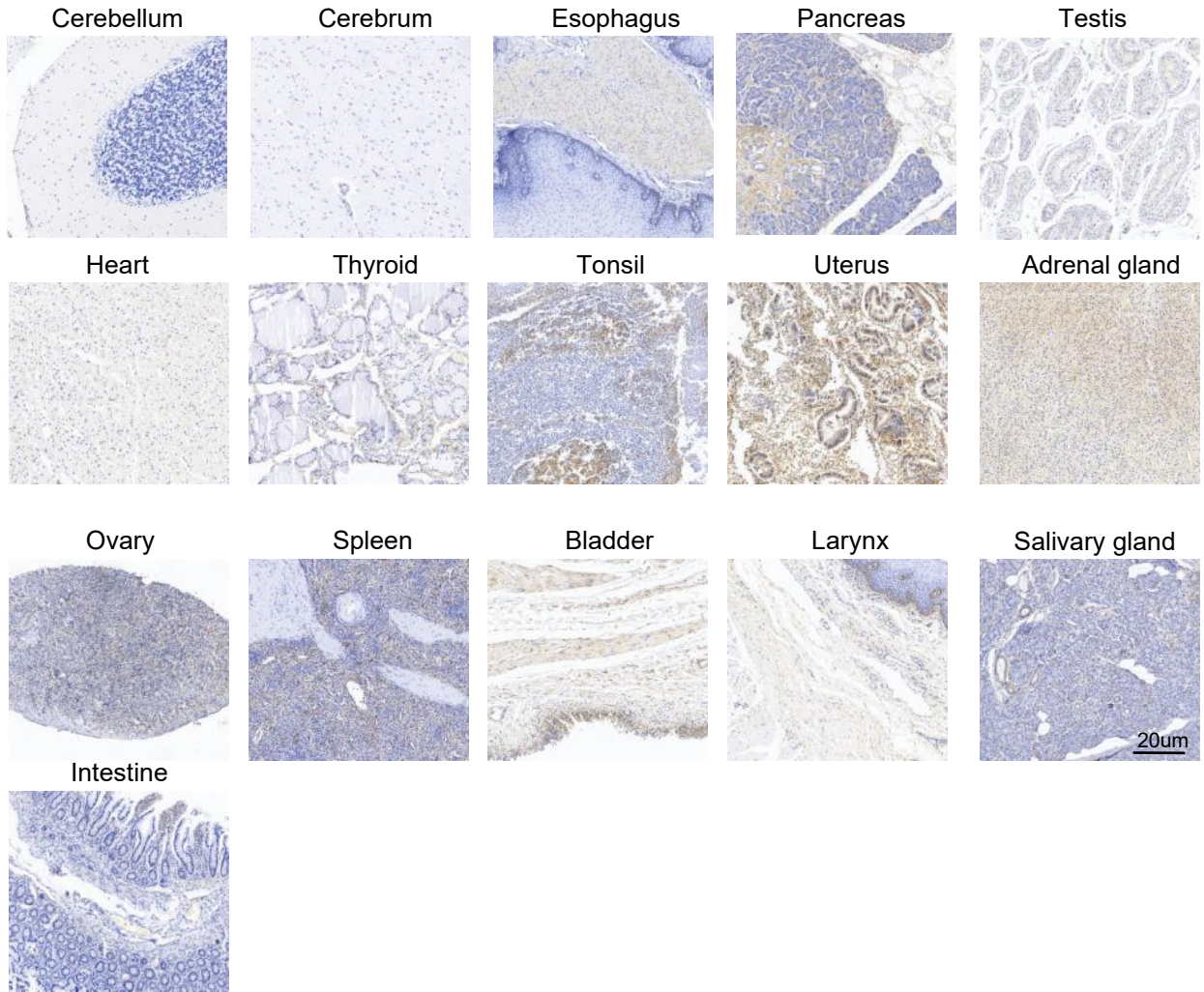


**Figure S4. IHC staining for B7-H3 expression in human normal tissues**

Representative IHC images of B7-H3 expression in human normal tissues including cerebellum, cerebrum, esophagus, pancreas, testis, heart, thyroid, tonsil, uterus, adrenal gland, ovary, spleen, bladder, larynx, salivary gland and intestine. Scale bars, 200 µm.

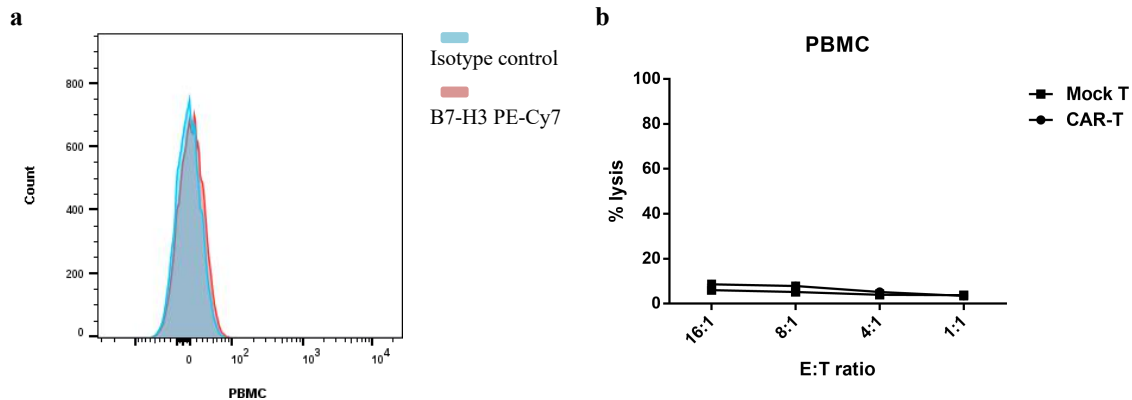


**Figure S5. Expression of B7-H3 in PBMCs and the cytotoxicity of CAR-T cells against PBMCs**

a. Expression of B7-H3 in PBMCs was evaluated by FACS. Cells were incubated with B7-H3-PE-Cy7 (purchased from BioLegend) (red) or its corresponding isotype control (blue).

b. <sup>51</sup>Cr-release assay to measure the cytotoxicity of CAR-T cells against PBMCs at different E:T ratios.